Pergamon

Int. J. Solids Structures Vol. 34, No. 21, pp. 2649–2668, 1997

0020–7683/97 $17.00 + .00

PII: S0020–7683(96)00179–5

STRENGTH AND RELIABILITY OF FIBER-REINFORCED COMPOSITES: LOCALIZED LOAD-SHARING AND ASSOCIATED SIZE EFFECTS

M. IBNABDELJALIL and W. A. CURTIN†
Department of Engineering Science & Mechanics and Materials Science & Engineering, Virginia Polytechnic Institute and State University, Blacksburg, VA 24061, U.S.A.

(*Received* 17 *November* 1995; *in revised form* 18 *February* 1996)

Abstract—The statistical aspects of the failure of large 3-D unidirectional fiber reinforced composites are studied numerically and analytically. A 3-D lattice Green's function model is used to calculate the stress field, damage evolution, and failure in composites under "Local Load Sharing" (LLS) conditions in which the stress from broken fibers is transferred predominantly to the nearby unbroken fibers. Failure by local accumulation of a critical amount of damage, and the associated decrease in ultimate strength with increasing composite size, is explicitly demonstrated. Weakest-link statistics are then employed to investigate size effects and reliability. An intrinsic "link" in LLS is found which has the same Gaussian distribution function for strength as a bundle in Global Load Sharing (GLS) (no local stress concentrations) of the same size. The size of the link is found to be comparable to the critical cluster of fiber damage observed in the simulations. Then, using known results for the GLS probability distribution function, analytic asymptotic results for the strength and reliability of large composites in LLS are derived. The strength distribution shows excellent agreement with the Monte Carlo simulation results for both the median strength and high reliability tail of the distribution. The implications of these results on the expected strength and reliability of moderate-size composites components is discussed, with applications to a Ti-MMC and a SiC/SiC CMC. Finally, the application of these results to modeling of composite failure by the Finite Element Method is presented. © 1997 Elsevier Science Ltd.

1. INTRODUCTION

The deformation and failure processes in 3-D unidirectional fiber reinforced composites are complex in nature, but involve a series of relatively well understood events, the details of which depend on the nature of the matrix. In brittle matrix composites such as ceramics, roughly equally spaced matrix cracks perpendicular to the fiber direction are usually the first non-linear event. In metal matrix composites, the matrix will plastically yield prior to failure. In polymer matrix composites the relatively low modulus of the matrix will exhibit a linear elastic behavior, but nearly all of the load is carried by the fibers. Thus, in all cases, as the load is increased beyond the matrix "yield" threshold, the fibers carry essentially all of the additional load. Further non-linear deformation then occurs as the fibers start breaking due to the presence of randomly distributed flaws in the fibers. The stress from the broken fibers is redistributed to the remaining fibers as determined by yield or debond/slip zones at the fiber/matrix interface. Distributed fiber failure continues in a stable manner until a cluster of fiber breaks reaches some critical size, triggering the catastrophic failure of the composite. Although the composite eventually separates along a single plane perpendicular to the direction of the fibers, the stochastic fiber failures usually occur at random distances away from the catastrophic plane, resulting in fiber pull-out. The distributed fiber breaks prior to failure tend to diffuse the stress concentrations at the perimeter of the clusters of fiber damage and so inhibit catastrophic failure. The extent and magnitude of the stress concentration around growing clusters of fiber breaks depends, however, on the fiber/matrix interface deformation and the statistics of fiber failure.

Several approaches have been taken previously to predict the tensile strength of unidirectional composites. These range from two and three dimensional Finite Element

† To whom all correspondence should be addressed.

Models (FEM) (Goree and Gross, 1980; Hikami and Chou, 1990; Goda and Phoenix, 1994), to shear-lag type model. Chou (1992) gives an extensive review of the various shear-lag models. Typically the finite element analyses tend to ignore the spatial variations of fiber break locations (fiber 'pull-out') and are limited to the analysis of small numbers of fibers. The inability to account for fiber pull-out leads to overestimates of the stress concentration at the crack tip and in turn underestimates composite strength. The shear-lag models have been quite popular because they allow for most of the physics of the problem to be retained and for the possibility of including the stochastic aspects of failure, while keeping the problem tractable. Previous Monte Carlo simulation techniques based on interpretation of the shear-lag model and constant interface shear stress assumptions (Curtin, 1993; Ibnabdeljalil, 1994; Ibnabdeljalil and Phoenix, 1995) and the analytic stochastic models (Thouless and Evans, 1988; Sutcu, 1989; Schwietert and Steif, 1990, 1991; Curtin, 1991; Phoenix, 1993; Neumeister, 1993; Ibnabdeljalil and Phoenix, 1995) for ceramic and metal matrix composites have been developed within the additional approximation of Global Load Sharing framework (GLS). GLS refers to the assumption that the stress from a broken fiber is distributed globally across all remaining intact fibers in the cross-section of the composite. The GLS model leads to the identification of key strength and length scales in the failure process, and has been shown to give good predictions for the strength of many ceramic matrix composites and Ti-metal matrix composites, but does not appear to apply to Al-metal or polymeric matrix composites. Also, GLS gives a rather idealized description of the stress transfer and should be considered an upper bound strength because there are no local stress concentrations. In practice the stress from a broken fiber is usually redistributed amongst a limited number of intact fibers, which makes some sort of Local Load Sharing (LLS) a more appropriate assumption for the failure process. Adopting the assumption of LLS results in higher stress concentrations due to broken fibers. Consequently, composites under LLS have lower strength and strain to failure, a distribution of strength that is much broader than for composites under GLS, a size dependence of strength, and notch sensitivity.

Two recent developments in the shear-lag type model which account for Local Load Sharing are the Break Influence Superposition Technique (BIS) (Sastry and Phoenix, 1993; Beyerlein and Phoenix, 1996) which is an extension of Hedgepeth's model (1961) and the more approximate formulation of the lattice Green's function technique adapted to composite failure by Zhou and Curtin (1995). Both the BIS and the Green's function technique are attractive for solving the composite failure problem since in both cases the size of the numerical problem to be solved is proportional to only the number of fiber breaks in the composite, in contrast to the FEM where the size of problem is the total volume of the composite. Using these new shear-lag techniques, relatively large composites can be analyzed numerically, up to several orders of magnitude larger than can be analyzed by the Finite Element Method. We will see below that this is important under Local Load Sharing because a weak-link type size scaling only sets in at larger composite sizes. Furthermore, in the Green's function method the extent of the load sharing is a parameter that can be chosen to obtain load sharing ranging from GLS to very LLS, where nearly all of the stress from broken fibers is redistributed on the nearest fibers only. This technique therefore provides a tool for studying the effects of the spatial range of load sharing on the various aspects of failure of composites with different types of matrices and interfaces.

In this paper, composite strength and its size dependence are investigated for composites with very local Load Sharing using a Monte Carlo simulation model based on the 3-D lattice Green's function technique, fully described in Zhou and Curtin (1995). Computer simulations are conducted on composite models on the scale slightly larger than a certain characteristic length δ_c and having up to 1600 parallel fibers arranged in a 3-D square array. We find that as the applied load on a composite is increased, clusters of damaged fibers form and grow until one of them reaches some critical cluster size and triggers the catastrophic failure of the composite. This weakest cluster of fiber breaks is then responsible for the composite failure, and each individual composite will have a different critical cluster and a different strength. To investigate failure of even larger composites, beyond the sizes that can be studied even with this efficient technique, we use weak-link scaling. Specifically,

we obtain the probability distribution functions for failure via simulation on moderate-size composites, demonstrate that weak-link scaling holds even at these sizes, and then use scaling techniques based on the weakest link approach, originally proposed by Gücer and Gurland (1962), to extrapolate the results to larger size composites.

In the failure process, we notice that just prior to failure, a composite in LLS exhibits a stress concentration around the perimeter of the critical cluster of fiber breaks that is relatively constant over a finite range extending away from the cluster. So, at that point, we can identify a small bundle within the composite which contains the critical cluster of fiber breaks, and the perimeter of near constant stress around it. We call it a "link". We postulate that the distribution function for the strength of such "link" is identical to the Gaussian distribution function of a same size link under Global Load Sharing, because just prior to failure, their stress states are identical. Another way to view this is that for a composite with some sufficiently small number of fibers, the damage at failure creates stresses in the remaining fibers that are essentially insensitive to the nature of the load sharing. In other words, we postulate that for a small size composite, Local and Global Load Sharing give identical results for the composite failure probability distribution. This postulate is then demonstrated explicitly by identifying a specific composite size (n_l fibers of length δ_l) for which Local and Global Load sharing are equivalent. Recent analytic results for the much simpler results for GLS can then be applied to LLS at this specific size. Weak-link scaling to obtain failure probabilities for a large composite in LLS is then performed analytically.

From this approach, we find that the LLS failure probability for composites follows a Weibull distribution with specific, analytic forms for the composite characteristic strength and composite Weibull modulus as a function of composite size. These powerful analytic results are then applied to predict composite strength and reliability in several real composite systems (a Ti-MMC and SiC/SiC CMC, for which LLS is expected to be applicable) and good agreement with experimental results is obtained.

Various other models based on a chain-of-bundles (weakest-link) model and under various load sharing rules have been proposed (Zweben, 1968; Scop and Argon, 1969; Zweben and Rosen, 1970; Argon, 1972; Harlow and Phoenix, 1979, 1981a,b; Smith 1982, 1983; Pitt and Phoenix, 1982, 1983; Phoenix and Smith, 1983; and Phoenix and Kuo, 1987; Duxbury and Leath, 1994). These models use very idealized load sharing rules where the stress concentration factor due to a sequence of r adjacent breaks is assumed, rather than elastically determined. Also, to keep the problem analytically tractable, the effects of pull-out are not included in these models. These earlier LLS models can be categorized into two broad techniques. (1) Recursion analysis of Harlow and Phoenix (1979, 1981a,b), and the more recent and powerful result of Duxbury and Leath (1994), which provides a simple framework for calculating the probability distribution for strength, and is extremely accurate. Even though these models only consider the simpler linear crack problem in one-dimensional random systems, they are very useful in evaluating the accuracy of other models, and in the case of Duxbury and Leath (1994), provide some useful size scalings. (2) Asymptotic analysis developed by Smith (1982, 1983) make certain assumptions for the lower tail of the probability distribution function for the strength of fibers, and obtain a limiting Weibull distribution for the strength of the composite. The main weakness of that model is that the accuracy of the resulting approximations cannot be evaluated directly. A comparison of the various asymptotic techniques is given in Phoenix and Smith (1983).

The current model is essentially of the asymptotic type, but does not suffer from the shortcomings of earlier models and the stringent assumptions needed to make those models tractable. The current model assumes that in the chain of bundle model, the underlying statistically independent and identically distributed unit is not a fiber element, as assumed in the previous asymptotic models, but is a bundle containing n_l fibers of length δ_l. Knowing the size of the link then allows us to determine the size of the cluster of fiber breaks which controls the strength of composite, related to the critical k^*-failure concept proposed in the idealized model of Smith (1982, 1983).

The remainder of this paper is organized as follows. In Section 2 we give the main assumptions of the current model for composite failure, including the statistical fiber model

and the key scaling parameters, and summarize the basic features of the discrete model which is the basis for the Monte Carlo model. In Section 3 we demonstrate explicitly the weak-link behavior through Monte Carlo simulation results. In Section 4 we adapt the statistics of composites under GLS to those of a composite under LLS to predict the strength of large size composites under LLS. We then apply our results to some specific examples in Section 5, and discuss further implications and applications of our results.

2. MODEL FOR THE COMPOSITE TENSILE FAILURE

The model of the composite and the Monte Carlo simulation procedure used here are identical to those of Zhou and Curtin (1995). Here we merely summarize the basic method and describe a few new features. The reader is referred to Zhou and Curtin (1995) for a full description of the model.

The model consists of a square array of n_f parallel fibers in a matrix, of radius r and Young's modulus E_f. The boundary conditions are periodic in the plane perpendicular to the fiber direction. The model assumes that the matrix has already reached its matrix damage state, i.e., multiply-cracked, as in ceramic matrix composites, plastically yielded, as in metal matrix composites, or very low modulus, as in polymer matrix composites. In all cases the net effect is the same: the fibers carry all of the additional load applied to the composite. Furthermore the fiber/matrix interface is assumed to be rather weak. The interface shear stress τ is then controlled by a debonded sliding interface, after debonding during matrix cracking or fiber fracture, or by shear yielding of the matrix. For tractability, τ is assumed to be constant in sliding/yielding zone. A consequence of the constant τ assumption is that around any fiber break the axial fiber stress recovers linearly with distance from the break, and attains the remote fiber stress σ at a "slip length" $l_f = r\sigma/2\tau$. Note that in a composite with some fiber breaks, σ is the stress in an intact (not broken and not slipping) fiber, which is always larger than the applied composite stress because of stress transfer from the broken fibers in the vicinity. Fiber breaks occur from pre-existing flaws randomly distributed along the fiber length. The average number of flaws in a fiber length L with strength less than or equal to stress σ is given by

$$\mathcal{N}(\sigma, L) = \frac{L}{L_0}\left(\frac{\sigma}{\sigma_0}\right)^{\rho}, \tag{1}$$

which is the usual Weibull model for single fiber strength. σ_0 is the characteristic (0.632 probability) strength of a fiber of length L_0 in a tension test, and $\rho > 0$ is the Weibull shape parameter describing the variability in strength.

In the failure process it is convenient to retain the normalizing scales for length and strength of the previous GLS model (Curtin, 1991), known as the characteristic length δ_c and stress σ_c, respectively, defined by

$$\sigma_c = \left(\frac{\sigma_0^{\rho}\tau l_0}{r}\right)^{1/(\rho+1)} \quad \text{and} \quad \delta_c = \left(\frac{\sigma_0 r l_0^{1/\rho}}{\tau}\right)^{\rho/(\rho+1)}. \tag{2}$$

Physically, δ_c is twice the slip length around a fiber break that is required to attain the characteristic stress σ_c, and so satisfies the relationship $\delta_c = r\sigma_c/\tau$. Simultaneously, σ_c is the characteristic strength of a fiber of length δ_c, i.e. $\mathcal{N}(\sigma_c, \delta_c) = 1$. In the remainder of this work all stresses are normalized with respect to the characteristic stress σ_c.

The composite described above is partitioned into a regular array of $N_x \times N_y \times N_z$ fiber elements, each of length $\bar{\delta}$ (see Fig. 1). The length $\bar{\delta}$ is the longitudinal discretization length in the simulation model and must satisfy $\bar{\delta} \ll \delta_c$. Random strengths sampled from a Weibull distribution at length $\bar{\delta}$ are then assigned to every fiber element, with $\bar{\sigma} = \sigma_c(\bar{\delta}/\delta_c)^{1/\rho}$ as the Weibull scale parameter at length $\bar{\delta}$. The partitioned composite is then modeled by a 3-D lattice of elastic springs with each fiber element represented by one tensile spring of modulus

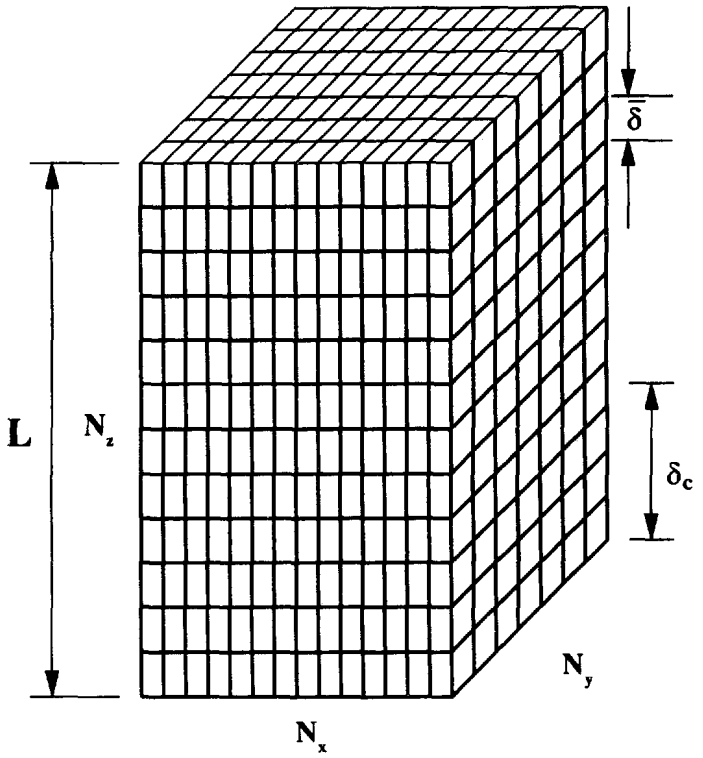

Fig. 1. Partitioned composite showing the various length scales.

k_f. Such 'fibers' are coupled to each other through orthogonal shear springs of shear modulus k_s. The tensile load bearing capacity of the matrix is essentially neglected at this stage, which is physically plausible when fiber failure controls composite failure. The ratio of shear to tensile modulus $\Omega^2 = k_s/k_f$ is an adjustable parameter in the simulation model. Varying Ω essentially changes the magnitude and extent of the load sharing: the limit $\Omega \to 0$ corresponds to the most extreme case of LLS in this model and is identical to the load sharing in the model of Hedgepeth and Van Dyke (1967) with a stress concentration of 1.14 on neighbors around a single broken fiber. $\Omega \to \infty$ corresponds to GLS. As noted by Zhou and Curtin (1995), Ω has not yet been directly related to the fiber, matrix, and interface material properties and the damage state of the matrix. In practice Ω can be determined as follows. Given the material properties of a particular system, the stress field around a broken fiber can be found using, for instance, a finite element analysis which includes matrix cracking and slipping or shear yield at the fiber/matrix interface as appropriate. Ω can then be chosen to match the stress concentration in the Green's function model to that of the finite element analysis. The resulting Ω is then used in the Monte Carlo simulation model to analyze much larger size composites with distributed damage. Though we will not attempt to make the connection between Ω and material properties in this paper explicitly, we are able to study the effects of varying Ω, and hence the spatial range of the load transfer, on the composite strength and reliability.

The Green's function technique of Zhou and Curtin (1995) determines the tensile stress field in such a model composite for any arbitrary configuration of broken fibers, and for a pre-selected load sharing rule (particular value of Ω). A Green's function is basically a response function $G_{i,j}$ which relates the displacement at a point i due to a unit point force applied at point j through $u_i = G_{i,j}F_j$. For an elastic (linear) system, Green's functions for any lattice structure are easily calculated. In the presence of broken springs in the lattice, modified Green's functions can also be calculated, requiring inversion of the matrix $G_{i,j}$, and the resulting stress distribution around the broken springs is then obtained directly. The model also includes inelastic fiber sliding associated with an interface sliding resistance τ by treating sliding fiber elements as "perfectly" plastic spring elements.

The algorithm for simulation of the tensile failure of the model composite using the above model is as follows. (1) An average stress equal to the strength of the weakest fiber element is applied to all elements. This causes the weakest element to break. (2) The stress at that point is set to zero and the stresses along the broken fiber within the slip length of the break are reduced to a stress proportional to the distance from the broken element (i.e., in the slip zone of a broken fiber the stress is given by $\sigma = 2\tau z/r$). (3) The stresses in all the other elements are calculated using the Green's function technique. (4) Fiber elements for which the stress exceeds their strength are identified, and we return to step (2). (5) If this is a stable configuration (i.e., stress at every fiber element is less than its strength), the applied stress per fiber is increased just enough to cause one additional element to break, and we return to step (2). The simulation continues until all fibers in any one layer of the composite are either broken or slipping; the composite can then no longer support the applied load. The applied stress just prior to failure is taken as the strength of the composite.

The simulation model of Zhou and Curtin (1995) has been improved significantly by incorporating very efficient techniques for inverting the Green's function matrix G_{ij}. We use the Sherman-Morrison and Woodbury algorithms (Press *et al.*, 1992) depending on the size of the problem. The Sherman-Morrison is the faster of the two algorithms but the need to store the entire matrix G_{ij} is a practical limitation. The Woodbury algorithm is the block-matrix version of the Sherman-Morrison and does not require the storage of the entire matrix G_{ij}.

3. MONTE-CARLO SIMULATION RESULTS

Zhou and Curtin (1995) demonstrated qualitatively that the failure of composites under LLS involves the formation of clusters of fiber damage. For relatively large composites these clusters seem to develop locally and independently of each other. Figures 2a,b show the critical cross section of a composite containing 400 fibers at failure for the cases of $\rho = 5$ and $\rho = 10$, respectively. In both cases, several small clusters and a dominant cluster of fiber damage are clearly identifiable. The "weakest" cluster is responsible for the final demise of the composite. Due to the localized nature of the failure process, we expect that as the number of fibers in the composite is increased, one can identify a region within a composite that is statistically representative of the rest of the composite, and therefore can be reviewed as a statistically independent entity. The composite is then only as strong as the weakest of these regions, which will be termed the "critical cluster". We therefore expect a weakest link behavior to emerge as the size of the composite is increased, one consequence of which is a dependence of strength on size.

To clearly illustrate these effects, Monte Carlo simulations are conducted for increasing numbers of fibers, $n_f = 100, 196, 400, 576, 900$, and a fixed length $2\delta_c$. The length $\bar{\delta}$ is chosen to be $\delta_c/20$ to minimize discretization errors and we choose a typical Weibull modulus $\rho = 5$. We also set the parameter $\Omega = 0.001$ which gives a very LLS, and is the most extreme case obtainable in this model and so provides the largest difference from the previous GLS model. Typically the probability distribution for the strength of a composite is based on approximately 1000 simulations for each composite size.

Figure 3 shows the probability distribution $\mathscr{H}_v(\sigma)$ for the strength of a composite plotted on Weibull coordinates $\ln(-\ln[1-\mathscr{H}_v(\sigma)])$ vs $\ln(\sigma)$ where σ is the composite strength normalized with respect to σ_c, and subscript v refers to the volume of the composite. As the number of fibers in the composite increases, the mean strength decreases, clearly demonstrating the size effect. For example, increasing the size from $n_f = 100$ to $n_f = 1600$ causes, in this particular case, a 3.2% drop in median strength. Also, the distribution function for strength becomes steeper suggesting an increase in reliability as n_f increases.

Now if the composite does follow a weakest link behavior, we can relate the distribution function for the strength at a composite of volume v_1 to that of a composite of volume v_2 through the weak-link scaling relationship

$$\mathscr{H}_{v_2}(\sigma) = 1 - [1 - \mathscr{H}_{v_1}(\sigma)]^{v_2/v_1}, \quad \sigma \geqslant 0. \tag{3}$$

Figure 4 shows attempts to weak-link scale distribution function for the strength of a

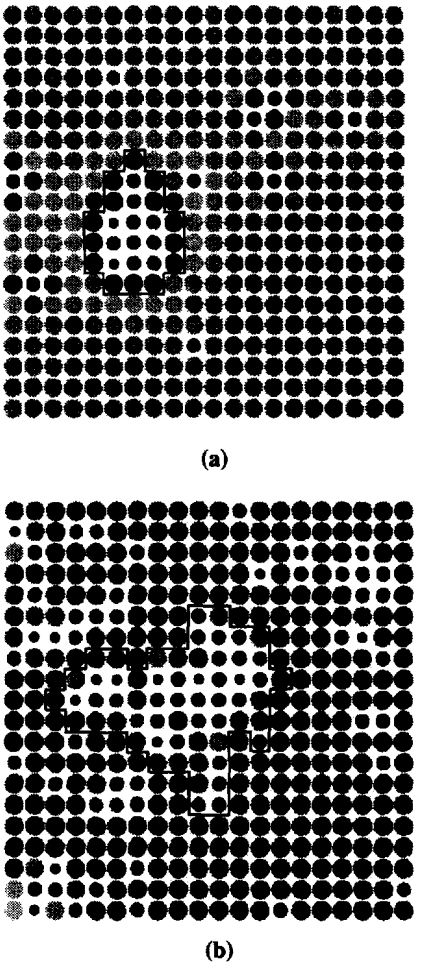

Fig. 2. Critical cross section of composite containing 400 fibers at failure. Box contains clustered broken and slipping fibers, and highly stressed fibers around that cluster. (a) $\rho = 10$, (b) $\rho = 5$.

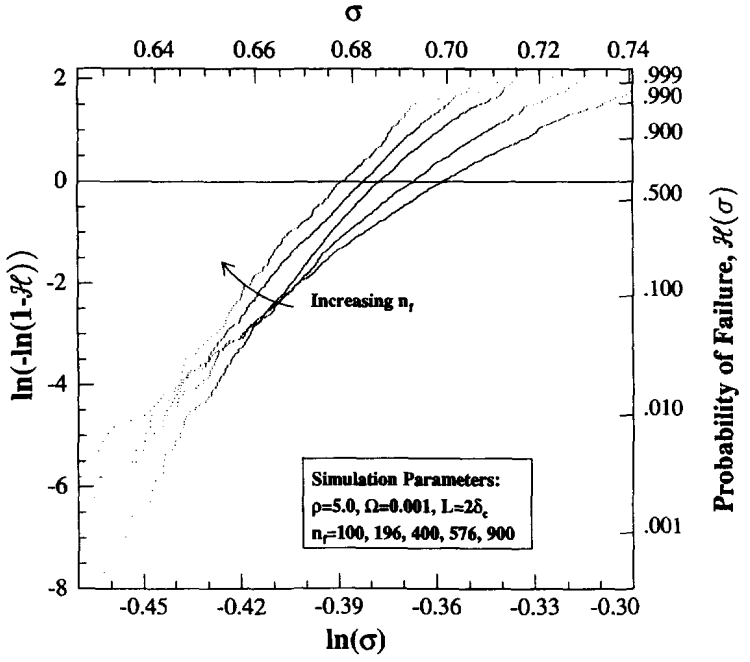

Fig. 3. Probability distribution for the strength of composites with increasing number of fibers, $n_f = 100, 196, 400, 576, 900$, and a fixed length $2\delta_c$, obtained through Monte Carlo simulation. The fiber Weibull modulus is $\rho = 5$. The distribution function is plotted on Weibull coordinates $\ln(-\ln[1-\mathscr{H}_c(\sigma)])$ vs $\ln(\sigma)$.

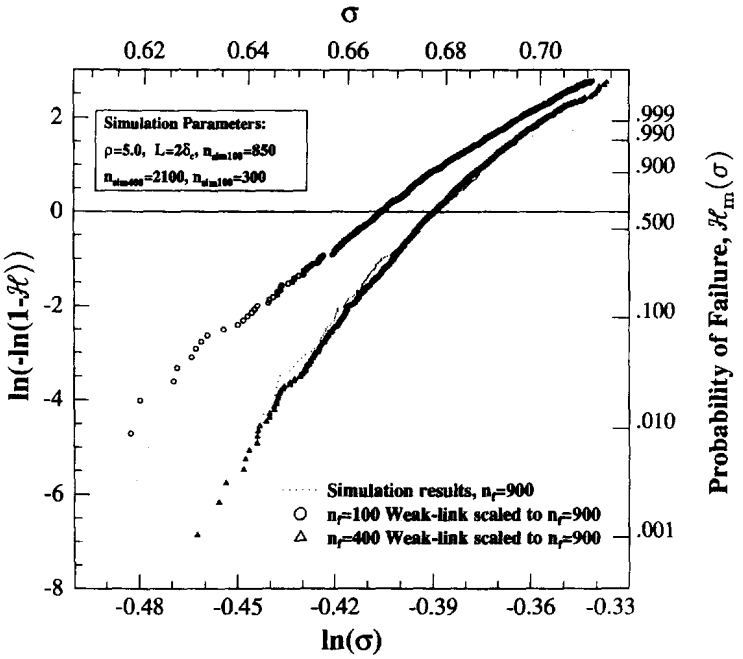

Fig. 4. Probability distribution function for the strength of composites obtained by weak link scaling the distribution function for strength of a simulated composite of size $n_f = 100$, and $n_f = 400$ to a composite of size $n_f = 900$. Also shown is the distribution function for strength obtained from simulating a composite of size $n_f = 900$. The distribution functions are plotted on Weibull coordinates. The Weibull modulus is $\rho = 5$.

composite of size $n_f = 100$ to $n_f = 900$, and size $n_f = 400$ to $n_f = 900$. In both cases the length of the composite is kept fixed at $L = 2\delta_c$. Figure 4 shows excellent agreement between the actual distribution obtained from simulation of a composite of size $n_f = 900$ and the extrapolated results from a composite of size $n_f = 400$, illustrating clearly the weak-link behavior. The rather poor agreement between the extrapolated results from a composite of size $n_f = 100$ and actual simulation strength results for $n_f = 900$ indicates that composite of size $n_f = 100$ is not large enough to account for correlations and boundary effects, and therefore cannot be used to extrapolate to larger size composites. There is some minimum size composite above which weak-link scaling applies and that minimum size varies with the load sharing parameter Ω and Weibull modulus ρ. Though not shown here, the cases $\rho = 10$ and $\rho = 2$ require a composite containing 600 fibers or more for weak-link scaling to set in for $\Omega = 0.001$. So for most Weibull moduli of practical interest (i.e., $2 \leqslant \rho \leqslant 10$) simulations should be conducted on composites $n_f \geqslant 600$ and $L \geqslant 2\delta_c$ to overcome correlation and boundary effects.

4. WEAK LINK SCALING AND THE STRENGTH DISTRIBUTIONS OF LARGE COMPOSITES

Having demonstrated the weakest link behavior explicitly by simulation, we will now take a more fundamental approach in tackling the size effect problem. Here are the main questions that need to be resolved. (1) Is there an underlying link size that is a fundamental unit for understanding the observed failure statistics and size scaling? (2) Is this size related to the critical clusters of fiber damage observed in the Monte Carlo simulations? (3) Are the statistics of such a link related to the statistics of a similar link under GLS?

We conjecture that the latter point is true, as proposed by Curtin (1993). Essentially, we believe that for a composite with a small number of fibers that the failure is insensitive to the nature of the load transfer. Since composites sustain a finite amount of damage in GLS, there are finite stress concentrations but they are distributed equally among all the fibers in the composite. In a small composite in LLS, damage leads to the stress concentrations which are initially highly heterogeneous but, as damage evolves in a small

composite, eventually becomes smeared over the entire (small) composite, leading to a situation very similar to that of GLS. This is certainly not the case for larger composites under LLS because isolated clusters with local stress concentrations certainly exist. To make a precise connection between LLS and GLS would then also allow us, at least from a mathematical point of view, to take full advantage of the known asymptotic results for Gaussian distribution of the GLS bundles and then to perform weak-link extrapolations analytically to obtain analytic predictions of the composite failure probability distribution.

The address these issues within a weakest link view point, the composite is modeled as a chain of statistically independent and identically distributed (i.i.d) links, the size and characteristics of which we wish to identify. We postulate that there does exist some intrinsic link, of length δ_l and containing n_l fibers in its cross-section, which controls failure of much larger composites. The link sizes δ_l, n_l will certainly depend on the extent of the load sharing, the statistically strength of the fibers, and the fiber/matrix interface properties. A large composite (length L and cross-section of n_f) is then considered to consist of mn of such links, where $m = L/\delta_l$ and $n = n_f/n_l$. The total number of links mn can range from 10^2 to 10^{10} in a practical size composite.

Next, let $\mathscr{G}_{n_l}(\sigma)$ be the probability distribution function for the strength of a link of size $n_l \cdot \delta_l$. Also, let $\mathscr{H}_{m,n}(\sigma)$ be the distribution function for a composite of mn such links. $\mathscr{H}_{m,n}(\sigma)$ has been obtained through the Monte Carlo simulations at various physical volumes $mn\delta_l n_l$ as shown, for example, in Fig. 3. According to the weakest link rule for statistically i.i.d links, $\mathscr{H}_{m,n}(\sigma)$ is related to $\mathscr{G}_{n_l}(\sigma)$ by

$$\mathscr{H}_{m,n}(\sigma) = 1 - [1 - \mathscr{G}_{n_l}(\sigma)]^{mn}, \quad \sigma \geqslant 0. \tag{4}$$

The distribution function $\mathscr{G}_{n_l}(\sigma)$ for the strength of a link and the link sizes n_l, δ_l are, *a priori*, not known but if such a link exists, it must satisfy eqn (4) for all the $\mathscr{H}_{m,n}(\sigma)$ which have been obtained through simulation.

We postulate that $\mathscr{G}_{n_l}(\sigma)$ is identical to the distribution for strength of the same size link in GLS. In GLS, the fundamental length of a link is $\delta_l = 0.4\delta_c$, as found by Phoenix *et al.* (1995), and is expected to be the same for LLS because the link length in the longitudinal direction should be independent of the transverse load sharing (aside from its connection to the characteristic length δ_c). We then search for the number of fibers n_l in the link so as to match the GLS distribution function $\Phi_{nl}(\sigma)$, which is a Gaussian distribution (Phoenix and Raj (1992)). That is, eqn (4) becomes

$$\mathscr{H}_{m,n}(\sigma) \approx 1 - [1 - \Phi_{n_l}(\sigma)]^{mn}, \tag{5}$$

where $\Phi_{n_l}(\sigma)$ is the Standard Gaussian distribution of the GLS bundle,

$$\Phi_{n_l}(\sigma) = \int_{-\infty}^{[\sigma - \mu^*_{n_l}]/\gamma^{**}_{n_l}} \frac{1}{\sqrt{2\pi}} \exp\left\{-\frac{x^2}{2}\right\} dx, \quad -\infty < \sigma < \infty. \tag{6}$$

$\mu^*_{n_l}$ and $\gamma^{**}_{n_l}$ are the normalized mean strength and standard deviation for the strength of a GLS bundle of length δ_l, respectively. Accurate approximations to $\mu^*_{n_l}$ and $\gamma^{**}_{n_l}$ are presented in the Appendix. The approximation to $\mathscr{H}_{m,n}(\sigma)$ given by eqn (5) will be referred to as the weak-linked Gaussian distribution.

To solve eqn (5) and determine the number of fibers in the link n_l we now use the concept of "reverse" weak-link scaling. That is, we write eqn (5) with $\Phi_{n_l}(\sigma)$ on the left-hand side

$$\Phi_{n_l}(\sigma) = 1 - [1 - \mathscr{H}_{m,n}(\sigma)]^{1/(mn)}. \tag{7}$$

The composite distribution function $\mathscr{H}_{m,n}(\sigma)$ has already been determined through Monte Carlo simulations for various composite sizes n_f at $L = 2\delta_c$, and $\Phi_{n_l}(\sigma)$ can be expressed

analytically through eqn (6). The problem then reduces to solving eqn (7) for n_l, with $n = n_f/n_l$ and $m = L/\delta_l$ (where L is the length of the simulated composite; here $L = 2\delta_c$, so $m = 5$) by graphically matching the right-hand side of eqn (7) to $\Phi_{n_l}(\sigma)$. Note that eqn (7) is not explicit in that n_l appears on both sides of the equation, and a solution is not assumed; rather, its existence verifies our underlying non-trivial postulate relating LLS to GLS.

As an illustration, we study the case $\Omega = 0.001$, and three Weibull moduli $\rho = 2$, 5 and 10. The simulation results for $\rho = 5$ and $n_f = 576$ and 900 are reversed weak-link scaled according to eqn (7), and we vary n_l until eqn (7) is satisfied as closely as possible (Fig. 5a). For $\rho = 5$ this procedure leads to an "intrinsic" link of $n_l = 54$ (and $\delta_l = 0.4\delta_c$). For $\rho = 10$ and 2, the matching procedure leads to the size of the "intrinsic" link as $n_l = 21$ and $n_l = 165$, respectively, with $\delta_l = 0.4\delta_c$ (see Figs 5b,c).

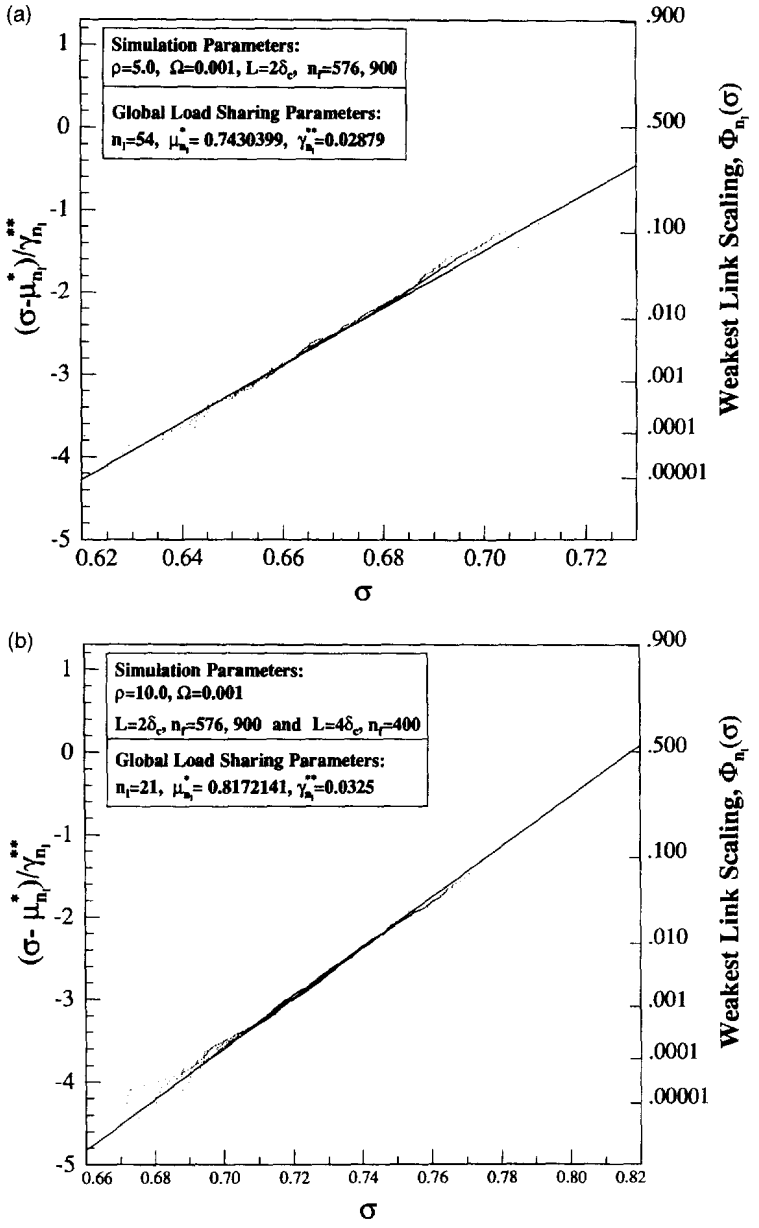

Fig. 5. Reverse weak link scaling of the strength of composites plotted on normal probability coordinates. Also shown are the analytic Gaussian distribution for the same link under GLS (solid lines). (a) Data for $n_f = 576{,}900$ and $L = 2\delta_c$ for $\rho = 5$, reverse weak linked to a link size $n_l = 54$ and $\delta_l = 0.4\delta_c$. (b) Data $n_f = 400$, 900 and $L = 2\delta_c$ for $\rho = 10$, reverse weak linked to a link size $n_l = 21$ and $\delta_l = 0.4\delta_c$. (c) Data $n_f = 400$ and $L = 2\delta_c$ for $\rho = 2$, reverse weak linked to a link size $n_l = 165$ and $\delta_l = 0.4\delta_c$. (*Continued opposite.*)

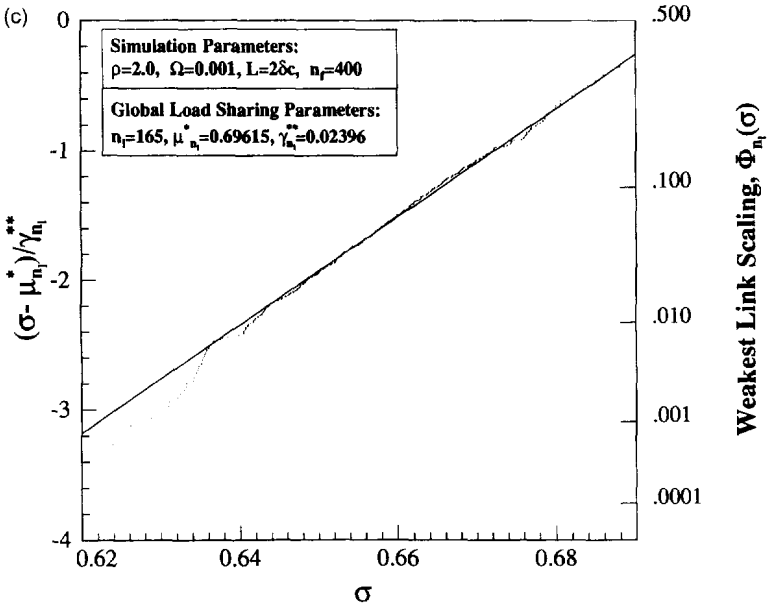

Fig. 5.—*Continued.*

We expect the link size n_l to be a function of the load sharing parameter Ω, such that $n_l = f(\rho, \Omega)$. It is beyond the scope of this work to map the full parameter space of n_l in terms of ρ and Ω. However, for the particular case of $\Omega = 0.001$ studied here, we find it useful to devise an empirical relationship between n_l and ρ from the simulations results,

$$n_l(\rho, \Omega)|_{\Omega=0.001} = 403\rho^{-1.28} \quad \text{for } 2 \leqslant \rho \leqslant 10. \tag{8}$$

It is not understood at this point how the fit parameters are connected to Ω, but the above relationship allows us to determined n_l for any $2 \leqslant \rho \leqslant 10$, without resorting to the lengthy simulations.

Having established a relationship between LLS and GLS at a particular size n_l, we note that there is evidence that the mathematically-derived link size corresponds in fact to a region containing the critical cluster of fiber damage at the onset of catastrophic failure and a perimeter of nearly constant stress around it. Figures 2a,b illustrate that connection, at least qualitatively, where counting the number of fibers in the failure plane and in the boxed region (the box contains clustered broken and slipping fibers, and highly stressed fibers around that cluster). For $\rho = 5$ and $\rho = 10$, the box contains 60 and 25 fibers, respectively, which are quite comparable to our intrinsic link sizes 54 and 21, respectively, obtained above. A more detailed study is needed, though, to prove the existence of a precise connection between n_l and the critical cluster, and should start with a careful definition of the "critical cluster" of fiber damage. This issue will be specifically addressed in our future work.

To reiterate our main result, we find that the strength distributions for large composites under LLS can be described by considering the composite to consist of a collection of size $n_l \cdot \delta_l$ links which have a strength distribution identical to that of $n_l \cdot \delta_l$ links under GLS; and analytic results for this $\Phi_{n_l}(\sigma)$ exist (see the Appendix). We have thus demonstrated unequivocally that it is possible to reduce the failure of a composite in LLS to that of a characteristic link in GLS. Below we discuss how to reap the benefits of all the asymptotic results developed for the GLS problem. The above results *do not* mean that one can, for example, simulate a composite of size $n_l = 54$ and $\delta_l = 0.4\delta_c$ in the case of $\rho = 5$, to obtain the statistics of the link. As pointed out in Section 3, simulated composites smaller than $n_f = 400$ do not give proper scaling for $\rho = 5$. Rather, simulations need to be carried out at larger sizes (say $L \geqslant 2\delta_c$ and $n_f \geqslant 400$ for $\rho = 5$) to minimize the correlations and

boundary effects and then analyzed as above to find the appropriate (and rather smaller) link size.

We are most interested in the distribution function $\mathscr{H}_{m,n}(\sigma)$ for composites much larger than can presently be studied numerically, but comparable to real composite sizes. The large number of links in a large size composite means that the behavior of $\mathscr{H}_{m,n}(\sigma)$ will be governed by the extreme lower tail ($\sigma \ll 1$) of the distribution function $\Phi_{n_l}(\sigma)$. We can thus take full advantage of the known asymptotic results for the strength of classical bundles from the theory of extremes. The distribution function $\mathscr{H}_{m,n}(\sigma)$ can then be approximated by a double exponential distribution (Smith and Phoenix, 1981; Smith, 1982). Phoenix and Raj (1992) also proposed a Weibull approximation to $\mathscr{H}_{m,n}(\sigma)$ that is more accurate than the double exponential approximation, and is conservative with respect to the "Exact" result of eqn (5). Furthermore, from a practical view point, using the Weibull approximation allows us to establish a direct connection between the fiber and composite Weibull parameters. The Weibull approximation to $\mathscr{H}_{m,n}(\sigma)$ has the form

$$\mathscr{H}_{m,n}(\sigma) \approx 1-\exp\left\{-\left(\frac{\sigma}{\tilde{\sigma}}\right)^{\tilde{\rho}}\right\}, \tag{9}$$

where the composite Weibull scale $\tilde{\sigma}$ and shape $\tilde{\rho}$ parameters are given by

$$\tilde{\sigma} = b_{m,n} \quad \text{and} \quad \tilde{\rho} = \frac{b_{m,n}}{a_{m,n}}. \tag{10}$$

$a_{m,n}$ and $b_{m,n}$ are in turn given by

$$a_{m,n} = \frac{\gamma^{**}_{n_l}}{\sqrt{2\log(m,n)}}, \tag{11}$$

and

$$b_{m,n} = \mu^{*}_{n_l} + \gamma^{**}_{n_l}\left[\frac{\log(\log(m\cdot n)) + \log(4\pi)}{\sqrt{8\log(m\cdot n)}} - \sqrt{2\log(m\cdot n)}\right]. \tag{12}$$

Recall that $\mu^{*}_{n_l}$ and $\gamma^{**}_{n_l}$ are the analytical mean and standard deviation for the strength of the intrinsic link of size $n_l\cdot\delta_l$, are defined in the Appendix, and are presented in Table 1 for

Table 1. Global Load Sharing results for the mean strength $\mu^{*}_{n_l}$ and standard deviation $\gamma^{**}_{n_l}$ for the intrinsic link of size $n_l\cdot\delta_l$, for various Weibull moduli ρ. The appropriate size n_l for each ρ is obtained from eqn (8), an empirical fit to the simulation data

ρ	n_l eqn (8)	$\mu^{*}_{n_l}$ eqn (A3)	$\gamma^{**}_{n_l}$ eqn (A6)
2.0	166	0.68687	0.02307
3.0	99	0.69961	0.02572
4.0	68	0.72563	0.02781
4.5	59	0.74149	0.02850
5.0	51	0.74416	0.02934
5.5	45	0.75161	0.02998
6.0	41	0.75945	0.03028
6.5	37	0.76763	0.03074
7.0	33	0.77596	0.03138
7.5	31	0.78318	0.03139
8.0	28	0.79090	0.03192
8.5	26	0.79788	0.03211
9.0	24	0.80474	0.03240
9.5	23	0.81062	0.03223
10.0	21	0.81727	0.03265

various Weibull moduli ρ. Also, recall that n and n_l are related by the relationship $n = n_f/n_l$. The asymptotic median strength of the composite is the value σ^* for which $\mathscr{H}_{m,n}(\sigma^*) = 1/2$, which is

$$\sigma^* = b_{m,n} + a_{m,n} \log(\log(2)). \tag{13}$$

The composite mean strength $\bar{\sigma}$ and standard deviation γ are also given in terms of $\tilde{\sigma}$ and $\tilde{\rho}$ by

$$\bar{\sigma} = \tilde{\sigma}\Gamma\left(1+\frac{1}{\tilde{\rho}}\right) \quad \text{and} \quad \gamma = \tilde{\sigma}\sqrt{\Gamma\left(1+\frac{2}{\tilde{\rho}}\right) - \Gamma\left(1+\frac{1}{\tilde{\rho}}\right)^2}, \tag{14}$$

where $\Gamma(\cdot)$ stands for the Gamma function.

We now test the Weibull approximation in eqn (9) against the simulation results and the weak-link Gaussian distribution in eqn (5) for the case $\Omega = 0.001$. Figures 6a and 6b show the scaled results for the case of $\rho = 5$ and $n_f = 576$, and 900, respectively. Figure 6c shows the scaled results for the case of $\rho = 10$ and $n_f = 900$. Both the weak-linked Gaussian and the Weibull approximation give equally impressive agreement at the median strength with the simulation results. As the number of fibers increases, the agreement at the median is even better. In the lower tail of the distribution function, the Weibull approximation gives the a more conservative estimate as the size of the composite is increased. This is important since the lower tail of the distribution corresponds to a stress level of high reliability.

Finally, we test the asymptotic median strength given by eqn (13) as a function of size of the composite. Recall that the distribution function for the strength of a large chain of links $\mathscr{H}_{m,n}(\sigma)$ is governed by the lower tail (or weakest link) of the distribution function for a single link $\Phi_{n_l}(\sigma)$, since a large composite is only as strong as its weakest link. This means that $\Phi_{n_l}(\sigma)$ contains statistical information about composites larger than the link itself, and this connection is explicit in eqn (5). To obtain the media strength at size mn, we set $\mathscr{H}_{m,n}(\sigma^*) = 1/2$ in eqn (5) and solve for σ^*. This leads to $\Phi_{n_l}(\sigma^*) = 1-(1/2)^{1(mn)}$, and so given mn one can read off the appropriate value of σ^* from the abscissa in Fig. 5. Figures 7a,b show the median strength obtained in this way versus composite size mn for $\rho = 5$, 10, respectively, from both the actual individual Monte Carlo simulation results and the analytic Weibull approximation of eqn (13), for different size composites. The agreement is again excellent between analysis and simulation for composites containing up to 10^4 links, which is an order of magnitude larger than the size that can be simulated directly. We have confidence that the prediction remains good for sizes $m \cdot n$ up to 10^8 links.

5. APPLICATIONS AND DISCUSSION

We first apply the current model to predict the strength of a unidirectional SCS-6 SiC fiber/Ti-24Al-11Nb composite fabricated via the powder-cloth method by MacKay *et al.* (1994). The interfacial shear stress used in the calculation is $\tau = 56$ MPa (Wawner, 1988; Brindley *et al.*, 1992) and we assume Local Load Sharing ($\Omega = 0.001$) for this case. Fiber strength was based on extracted fibers from composite panels, and is modeled by a two-parameter Weibull distribution with Weibull modulus $\rho = 8.6$. The fiber strength, based on a gauge length $l_0 = 12.7$ mm, is $\sigma_0 = 4577$ MPa and the fiber diameter is $d = 142$ μm. The average volume fraction of fibers is $f = 0.26 \pm 0.028$, and the matrix yield stress is $\sigma_{my} \approx 546$ MPa (Brindley *et al.*, 1992). The constituent material properties are summarized in the top half of Table 2. In calculating the Ultimate Tensile Strength (UTS) of a metal matrix composite, it is necessary to add the tensile contribution of the yielding matrix, so that

$$\text{UTS} = \bar{\sigma} f + \sigma_{my}(1-f), \tag{15}$$

where σ_{my} is the yield stress of the matrix material, $\bar{\sigma}$ is given by eqn (14) and f is the fiber volume fraction. The stochastic nature of composite failure is mainly governed by the statistical nature of fiber strength, so the standard deviation for the composite is taken as the standard deviation for the fiber bundle γ is given by eqn (14). Experimentally, a coupon of length $L_0 = 25.4$ mm, width $w = 6.35$ mm and thickness $t = 1.3$ mm was found to have a mean ultimate tensile strength of 1251 ± 93 MPa (MacKay *et al.*, 1994). In our analysis, the link size is $\delta_l = 0.4\delta_c$ where $\delta_c = 6.29$ mm (given by eqn (2)), and $n_l = 26$ obtained from eqn (8). The coupon thus has a total of $mn = 53$ statistically independent links. Equations

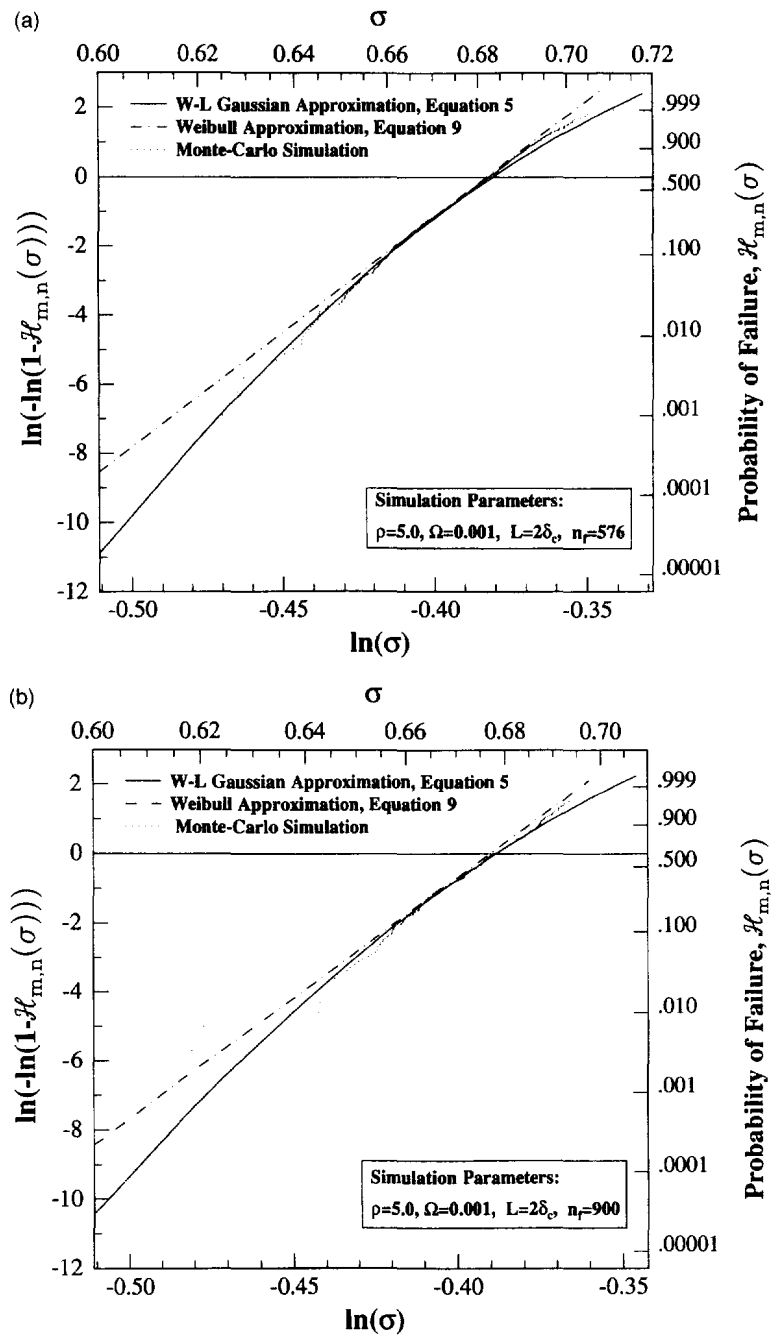

Fig. 6. Distribution function for the strength of composites plotted on Weibull probability coordinates. Shown are the scaled composite strengths for the case (a) $\rho = 5$, $n_l = 576$, $m = 5$, and $n = 10.67$, (b) $\rho = 5$, $n_l = 900$, $m = 5$, and $n = 16.67$, and (c) $\rho = 10$, $n_l = 900$, $m = 5$, and $n = 42.86$. Also shown for each case are the weak linked Gaussian approximation of eqn (5) and the Weibull approximation given by eqn (9). (*Continued opposite.*)

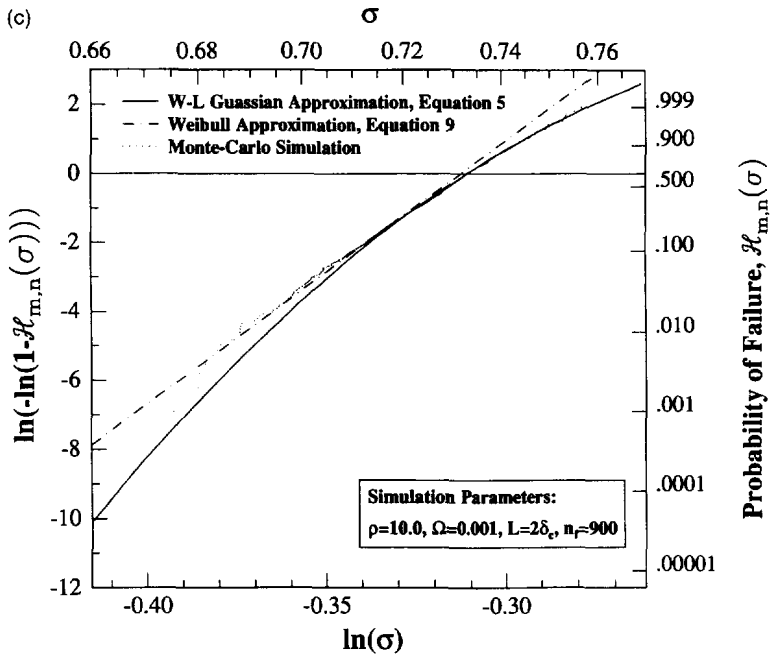

Fig. 6.—*Continued.*

(10)–(14) then predict that the ultimate tensile strength is 1338 ± 71 MPa. Using eqns (A3) and (A6) in the Appendix with n_l set to n_f, the GLS analysis, on the other hand, yields a higher UTS of 1387 ± 46 MPa. The discrepancy between the experimental results and the LLS analysis is only 7% for the strength of the composite, compared with 11% for the GLS analysis (using eqns (A3) and (A6) in the Appendix, with n_l set to n_f), and is partly attributable to several factors: (1) approximating the fiber strength distribution with a two parameter Weibull distribution, (2) the values of τ and σ_{my} used in the analysis are only estimates, (3) the uncertainty of 2.8% in the volume fraction of fibers: choosing the lower-end and upper-end estimates for f (i.e., $f = 0.232$ and $f = 0.288$, respectively) yield mean ultimate tensile strengths of 1254 MPa and 1422 MPa, and finally, (4) the present analysis does not take into account the effects of processing and/or handling induced damage which is invariably present in real composites, as discussed by Duva *et al.* (1995). Including the latter effects in the analysis, using an approach similar to that taken by Ibnabdeljalil and Phoenix (1995), or Curtin and Zhou (1995) should lower the ultimate tensile strength and increase the variability, moving in the right direction for a closer match between the experimental results and analytic prediction. Though the effects of the various estimates and approximations, apart from f, are not quantified specifically, their net effect on composite strength is expected to be quite small (in the absence of extensive processing damage) and, in all, the analytic prediction for strength is remarkably good. Note that the relatively small difference between the LLS and GLS analysis for this particular composite system, at the coupon size, is expected due to the relatively small number of fibers in the cross-section. The difference between the two analyses is expected to grow rapidly as the size of the composite is increased. To illustrate the predicted size effect and its importance to composite performance, we increase the size of the composite from a coupon (24.5 mm × 6.35 mm × 1.3 mm) to a "panel" (1000 mm × 1000 mm × 1.3 mm), which contains 326,398 links. Such an increase in size results in an 8.3% decrease in the LLS predicted mean strength (UTS = 1235 MPa) but an 82% decrease in the standard deviation ($\gamma = 39$ MPa).

Next we apply the model to predict the strength of SiC-SiC fiber reinforced composite coupons and components fabricated by the CVI method. The Nicalon SiC fibers have a diameter $d = 16$ μm and Weibull modulus $\rho = 4.5$. The sliding resistance is $\tau = 100$ MPa and the *in situ* fiber characteristic strength is $\sigma_c = 1.5$ GPa (Evans and Zok, 1994), giving a characteristic length $\delta_c = 120$ μm. The fiber volume fraction used is $f = 0.2$. The constituent

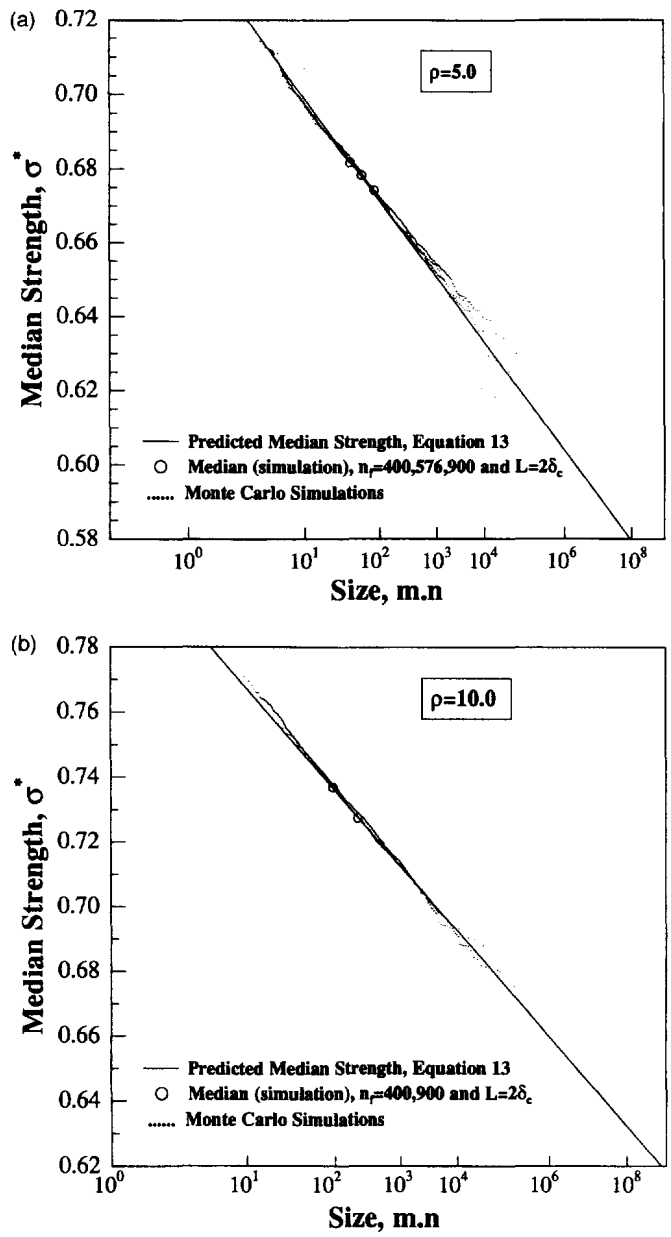

Fig. 7. Median strength vs composite size mn obtained from both the Weibull approximation and the actual individual Monte Carlo simulation results. (a) $\rho = 5$, $n_f = 54$, and (b) $\rho = 10$, $n_f = 21$.

Table 2. Constituent material properties and composite ultimate tensile strength for SCS-6 SiC fiber/Ti-24Al-11Nb matrix and SiC-SiC composites.

Constituent material properties	SCS-6 SiC fiber/Ti-24Al-11Nb matrix	SiC-SiC composite
Interface stress τ (MPa)	56	100
Fiber diameter d (μm)	142	16
Fiber strength σ_0 (MPa) based on l_0	4577	—
Fiber Gauge length l_0 (mm)	12.7	—
Fiber Weibull Modulus ρ	8.6	4.5
Fiber Characteristic Stress σ_c (GPa)	4.97	1.50
Fiber Characteristic length δ_c (mm)	6.29	0.12
Fiber Volume fraction f	0.26 ± 0.028	0.2
Matrix yield strength σ_{my} (MPa)	546	—
Composite Tensile Strength	Coupon	Coupon
Measured (MPa)	1251 ± 93	157
Predicted (eqns (10)–(14)) (MPa)	1338 ± 71	182 ± 11

material properties are summarized in the top half of Table 2. In our LLS analysis, we use a link size $\delta_l = 0.4\delta_c$, and $n_l = 59$ obtained from eqn 8. A coupon of size 24.5 mm × 6.35 mm × 1.3 mm then has a total of 3.6×10^5 statistically independent links. Equations (10)–(14) then predict that the UTS is 182 ± 11 MPa, whereas the GLS (using eqns (A3) and (A6) in the Appendix, with n_l set to n_f) applied to the composite yields a UTS of 212 ± 2 MPa. The experimentally measured UTS is 157 MPA, so the discrepancy between the experimental and predicted UTS from LLS and GLS analyses are 16% and 35%, respectively. The LLS model fairs much better at predicting the strength of the SiC-SiC composites than the GLS model. The discrepancy between the LLS and experimental results may be due to the various estimates for the mechanical properties of the constituent materials and fiber volume fraction, but further investigation is needed. To illustrate the predicted size effects on the strength of SiC-SiC composites, we increase the size of the composite from a coupon (24.5 mm × 6.35 mm × 1.3 mm) to a "panel" (1000 mm × 1000 mm × 1.3 mm), which contains 1.1×10^9 links. Such an increase in size results in a further 7% decrease in the mean strength (UTS = 170 MPa) and a 32% decrease in the standard deviation ($\gamma = 8.4$ MPa). Moreover, the larger composites tend to exhibit a more brittle failure behavior than smaller composites, as evident from the shorter non-linear region in the stress-strain curve shown in Fig. 8.

We also apply our model to predict the UTS of a SiC-SiC tubular component (Curtin *et al.*, 1995) that has a length $L = 203.2$ mm, inner and outer diameters $r_i = 12.7$ mm and $r_o = 15.85$ mm, respectively. The 0° tow volume fraction used in the calculation is $f = 0.16$. The total number of links in the composite is 1.63×10^7. The LLS model predicts a UTS of 141 ± 9 MPa whereas the GLS analysis (using eqns (A3) and (A6) in the Appendix, with n_l set to n_f) applied to the full composite yields a UTS of 169 ± 0.26 MPa, or 20% higher strength than the LLS prediction. Experimentally, only one tube was tested and the UTS was found to be 139 MPA. Though limited, the experimental results do suggest that the LLS model is better at predicting the strength of a moderate size SiC-SiC composite component than the GLS model. It should be noted that using $\Omega = 0.001$ which is assumed, rather than derived, gives a load sharing that is very likely more local than the actual load sharing in the real composite.

A very useful application of the strength distribution we have obtained for statistically independent links is in the modeling composite failure using the Finite Element Method (FEM). In such models, the composite is treated as a homogeneous continuum, but with finite elements containing all the micro-mechanical information through a non-linear

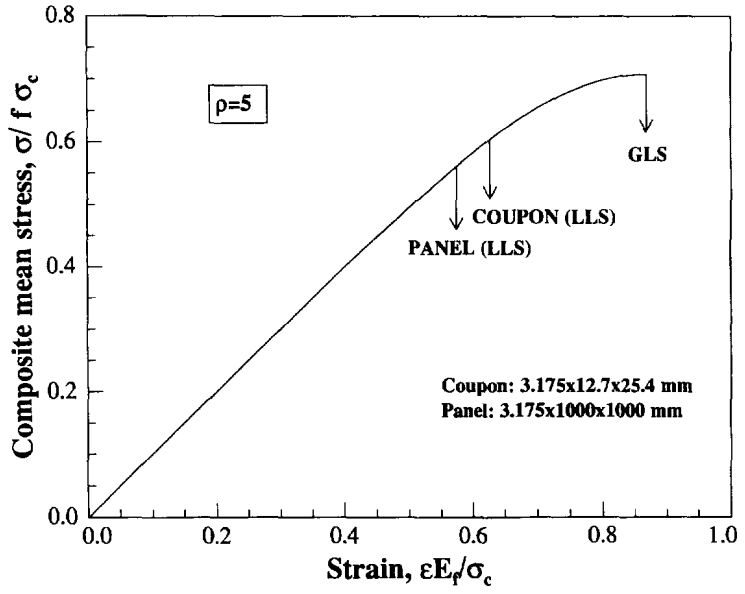

Fig. 8. Dimensionless Stress-Strain curves, $\sigma/f\sigma_c$ vs $\varepsilon E_f/\sigma_c$, for a SiC-SiC fiber reinforced composite, for two different sizes: coupon (24.5 mm × 6.35 mm × 1.3 mm), panel (100 mm × 1000 mm × 1.3 mm) (fiber bundle contribution only).

constitutive model based on the GLS theory for the deformation. Exact and approximate expressions for the stress-strain behavior of GLS bundles can be found in the literature (Hui *et al.*, 1995; Sutcu, 1989; Curtin, 1991; Neumeister, 1993; Phoenix, 1993). The finite elements are generally of different sizes as determined in the initial mesh distribution. However, the present results demand that the *minimum* element size correspond to several hundred fibers and a physical length $\geqslant 2\delta_c$ because composites smaller than such a size do not give proper scaling since they are not truly statistically independent. Care must be taken to make sure that the elements in the finite element mesh are large enough to realize this statistical independence. Having properly "meshed" the composite, the weak-link scaling approach is then used to determine the proper strength of each element consistent with its physical volume. Specifically, an element of n_f fibers and length L consists of $m \cdot n$ links of size $n_l \cdot \delta_l$ such that $mnn_l \delta_l = n_f L$. n_l is determined from results such as those above for the desired ρ and Ω, that is $n_l(\rho, \Omega)$. Lastly, a random number x in the interval [0, 1] is selected and the element is assigned the strength σ satisfying $\mathscr{H}_{m,n}(\sigma) = x$ where $\mathscr{H}_{m,n}(\sigma)$ is calculated from eqn (9). This approach is quite straight forward but guarantees proper handling of the statistics in assigning strengths to the finite elements and only uses the mechanical properties of the constituent materials as input parameters.

In future work, we will study more carefully the critical clusters which cause failure and the composite notch sensitivity. Specifically, we will determine how an initial cluster of fiber damage competes with the critical cluster formed on loading from the existing fiber flaw population (dictated by ρ), in causing the final collapse of the composite. The initial damage clusters may be un-bridged (notched) or bridged; the bridging is accomplished by assuming that the initial fiber breaks are randomly distributed a small distance away from some reference plane. We can then study the composite failure strength and reliability as a function of the size of this well defined initial cluster of fiber damage. Finally, note that Figs 4a,b,c show that as ρ increases (less variability in the fibers) the critical cluster size decreases, which means that a composite becomes much more vulnerable to local damage. Another way to view this is that the composite under LLS is more notch sensitive for higher fiber Weibull moduli.

In summary, we have demonstrated the weak-link nature of composite failure under Local Load Sharing and described how to map the reliability of a composite under Local Load Sharing to that of an intrinsic composite link under Global Load Sharing. The size of the link was found to be a function of the load sharing and the Weibull modulus. The statistical theory of extremes was then used to extrapolate the strength results for the link to composites much larger than can be analyzed using the Monte Carlo simulation model. The model was used to predict the strength of SiC/Ti-24Al-11Nb composite coupons and SiC-SiC composite coupons and components and showed generally good agreement with experimental results. The strength and reliability of many other fiber reinforced composites are approachable using this general technique if the appropriate load sharing parameter Ω can be determined (Du and McMeeking, 1993; Nedele and Wisnom, 1994). Our future effort will be directed toward obtaining the dependence of Ω on the underlying fiber, matrix, and interface constitutive properties so that such investigations can be carried out. We will also investigate the effects of both localized and random processing damage on the strength and reliability of fiber reinforced composites.

Acknowledgments—This research was supported by the U.S. Air Force Office of Scientific Research, Grant # F49620-95-1-0158. The authors would also like the thank S. L. Phoenix for some useful written comments.

REFERENCES

Argon, A. S. (1972) Fracture of composites. In *Treatise on Material Science and Technology* (ed. H. Herman), pp. 79–114. Academic Press, New York.

Beyerlein, I. J. and Phoenix, S. L. (1996) Stress concentrations around multiple fiber breaks in an elastic matrix with local yielding or debonding using quadratic influence superposition. *Journal of Mechanics, Physics and Solids*, (in press).

Brindley, P. K., Draper, S. L., Eldridge, J. I., Nathal, M. V. and Arnold, S. M. (1992) The effect of temperature on the deformation and fracture of SiC/Ti-24Al-11Nb. *Metallurgy and Material Transactions A* **34**, 2527–2540.

Chou, T. W. (1992) *Microstructural Design of Fiber Composites*. Cambridge University Press, U.K.

Curtin, W. A. (1991) Theory of mechanical properties of ceramic matrix composites. *Journal of the American Ceramic Society* **74,** 2837–2845.
Curtin, W. A. (1993) The tough to brittle transition in brittle matrix composites. *Journal of Mechanics, Physics and Solids* **41,** 217–245.
Curtin, W. A., Oleksuk, L. I., Reifsnider, K. L. and Stinton, D. P. (1995) Mechanical properties of ceramic composite tubes. In *Proc. Ninth Annual Conference on Fossil Energy Materials*, Oak Ridge, Tennessee, pp. 31–39.
Curtin, W. A. and Zhou, S. J. (1995) Influence of processing damage on the performance of fiber-reinforced composites. *Journal of Mechanics, Physics and Solids* **43,** 343–363.
Du, Z.-Z. and McMeeking, R. M. (1993) Control of strength anisotropy of metal matrix fiber composites. *Journal of Computer Aided Material Design* **1,** 243–264.
Duva, J. M., Curtin, W. A. and Wadley, H. N. G. (1995) An ultimate tensile strength dependence on processing for consolidated metal matrix composites. *Acta Metallurgica* **43,** 1119–1126.
Duxbury, P. M. and Leath, P. L. (1994) Failure probability and average strength of disordered systems. *Physical Review Letters* **72,** 2805–2808.
Evans, A. G. and Zok, F. W. (1994) The physics and mechanics of fiber-reinforced brittle matrix composites. *Journal of Material Science* **29,** 3857–3896.
Feller, W. (1968) An introduction to probability theory and its applications. In *Wiley Series in Probability and Mathematical Statistics* 3rd ed., bf 1, 174–179. John Wiley and Sons, Inc. New York.
Goda, K. and Phoenix, S. L. (1994) Reliability approach to the tensile strength of unidirectional CFRP composites by Monte-Carlo simulation in a shear-lag model. *Composite Science and Technology* **50,** 457–468.
Goree, J. G. and Gross, R. S. (1980) Stresses in a three-dimensional unidirectional composite containing broken fibers. *Engineering Fracture Mechanics* **13,** 395–405.
Gücer, D. E. and Gurland, J. (1962) Comparison of the statistics of two fracture modes. *Journal of Mechanics, Physics and Solids* **10,** 365–373.
Harlow, D. G. and Phoenix, S. L. (1979) Bounds on the probability of failure of composite materials. *International Journal of Fracture* **15,** 321–336.
Harlow, D. G. and Phoenix, S. L. (1981) Probability distributions for the strength of composite materials. I: Two level bounds. *International Journal of Fracture* **17,** 347–372.
Harlow, D. G. and Phoenix, S. L. (1981) Probability distributions for the strength of composite materials. II: A convergent sequence of tight bounds. *International Journal of Fracture* **17,** 601–630.
Hedgepeth, J. M. and Van Dyke, P. (1967) Local stress concentrations in imperfect filamentary composite materials. *Journal of Composite Materials* **1,** 294–309.
Hedgepeth, J. M. (1961) Stress concentration in filamentary structures. *NASA TN D-882*, NASA report, U.S.A.
Hikami, F. and Chou, T. W. (1990) Explicit crack problem solutions of unidirectional composites: Elastic stress concentrations. *AIAA Journal* **28,** 499–505.
Hui, C.-Y., Phoenix, S. L., Ibnabdeljalil, M. and Smith, R. L. (1995) An exact closed form solution for the fragmentation of Weibull fibers in a single filament composite with application to fiber reinforced ceramics. *Journal of Mechanics, Physics and Solids* **43.**
Ibnabdeljalil, M. (1994) Statistical aspects of the failure of brittle matrix composites, reinforced with unidirectional continuous, discontinuous, and time dependent brittle fibers. Ph.D. thesis, Cornell University, U.S.A.
Ibnabdeljalil, M. and Phoenix, S. L. (1995) Scalings in the statistical failure of brittle matrix composites with discontinuous fibers: analysis and Monte Carlo simulations. *Acta Metallurgica Materials* **43,** 2975–2983.
MacKay, R. A., Draper, L. S., Ritter, A. M. and Siemers, P. A. (1994) A comparison of the mechanical properties and microstructures of Intermetallic matrix composites fabricated by two different methods. *Metallurgy and Materials Transactions. A.* **25A,** 1443–1455.
McCartney, L. N. and Smith, R. L. (1983) Statistical theory of the theory of the strength of fiber bundles. *Journal of Applied Mechanics* **105,** 601–630.
Nedele, M. R. and Wisnom, M. R. (1993) Three-dimensional finite element analysis of the stress concentration at a single fibre break. *Composites Science and Technology* **51,** 517–524.
Neumeister, J. M. (1993) A constitutive law for continuous fiber reinforced brittle matrix composites with fiber fragmentation and stress recovery. *Journal of Mechanics, Physics and Solids* **41,** 1383–1404.
Phoenix, S. L. and Smith, R. L. (1983) A comparison of the probabilistic techniques for the strength of fibrous materials under local load-sharing among fibers. *International Journal of Solids and Structures* **19,** 479–496.
Phoenix, S. L. and Kuo, C.-C. (1987) Recursions and limit theorems for the strength and lifetime distributions of fibrous composites. *Journal of Applied Probability* **24,** 137–159.
Phoenix, S. L. and Raj, R. (1992) Scalings in fracture probabilities for a brittle matrix fiber composite. *Acta Metallurgica and Materials* **40,** 2813–2828.
Phoenix, S. L. (1993) Statistical issues in the fracture of brittle matrix fibrous composites. *Composite Science and Technology* **48,** 65–80.
Phoenix, S. L., Ibnabdeljalil, M. and Hui, C.-Y. (1995) Size effects in the distribution for strength of brittle matrix composites: Analysis and Monte-Carlo Simulation. *International Journal of Solids and Structures* (submitted).
Pitt, R. E. and Phoenix, S. L. (1982) Probability distributions for the strength of composite materials, III: the effect of fiber arrangement. *International Journal of Fracture* **20,** 291–311.
Pitt, R. E. and Phoenix, S. L. (1983) Probability distributions for the strength of composite materials, IV: Localized load-sharing with tapering. *International Journal of Fracture* **21,** 243–276.
Press, W. H., Teukolsky, S. A., Vetterling, W. T. and Flannery, B. P. (1992) *Numerical Recipes*, 2nd ed. Cambridge University Press, U.K.
Sastry, A. M. and Phoenix, S. L. (1993) Load redistribution near non-aligned fiber breaks in a two-dimensional unidirectional composite using break-influence superposition. *Journal of Material Science Letters* **12,** 1596–1599.
Schweitert, H. R. and Steif, P. S. (1990) A theory for the ultimate strength of brittle-matrix composites. *Journal of Mechanics, Physics and Solids* **38,** 325–343.
Schweitert, H. R. and Steif, P. S. (1991) On the tensile strength of a fiber reinforced ceramic. *Journal of Mechanics, Physics and Solids* **28,** 299–315.

Scop, P. M. and Argon, A. S. (1969) Statistical theory of strength of laminated composites II. *Journal of Composite Materials* **3,** 30–47.
Smith, R. L. and Phoenix, S. L. (1981) Asymptotic distribution for the failure of fibrous materials under series-parallel structure and equal load-sharing. *Journal of Applied Mechanics* **103,** 75–82.
Smith, R. L. (1982) The asymptotic distribution of the strength of a series-parallel system with equal load-sharing. *Annals of Probability* **10,** 137–171.
Smith, R. L. (1983) Limit theorems and approximations for the reliability of load-sharing systems. *Advances in Applied Probability* **15,** 304–330.
Sutcu, M. (1989) Weibull statistics applied to fiber failure in the ceramic composites and work of fracture. *Acta Metallurgica* **37,** 651–661.
Thouless, M. D. and Evans, A. G. (1988) Effects of pullout on the mechanical properties of ceramic-matrix composites. *Acta Metallurgica* **36,** 517–522.
Wawner, F. E. (1988) In *Fiber Reinforcements for Composite Materials*, (ed. Bunsell A. R.) Elsevier, NY, pp. 371–425.
Zhou, S. J. and Curtin, W. A. (1995) Failure of fiber composites: a lattice Green function Model. *Acta Metallurgica Materials* **43,** 3093–3104.
Zweben, C. (1968) Tensile failure analysis of fibrous composites. *AIAA Journal* **6,** 2325–2331.
Zweben, C. and Rosen, B. W. (1970) A statistical theory of the strength with application to composite materials. *Journal of Mechanics, Physics and Solids* **18,** 189–206.

APPENDIX

Here we outline some of the most recent results regarding the strength and standard deviation of a characteristic bundle in the GLS frame work.

An accurate approximation to the strength of a bundle can be obtained be taking the 3 term expansion of Hui *et al.*'s (1995) exact solution

$$\mu^* \approx s^* \left[1 - \frac{s^{*\rho+1}}{2} + \theta \frac{s^{*2\rho+2}}{24}\right] \exp\left\{-s^{*\rho-1}\left(1 - \lambda \frac{s^{*\rho+1}}{8}\right)\right\} \tag{A1}$$

where $\theta = (7\rho+12)/(2\rho+3)$ and $\lambda = \rho/(\rho+1)$. s^* is the fiber stress at the onset of composite collapse. An approximation for s^* was given by Phoenix *et al.* (1995) which was shown to be very accurate for all values of the Weibull modulus ρ,

$$s^* = \left[\left(\frac{2}{\rho}\right)\left(\frac{4\rho+2}{4\rho+1}\right)\right]^{1/(\rho+1)}. \tag{A2}$$

We include the correction Δ_{nl} to the asymptotic mean stress for small number of fibers in the link,

$$\mu^*_{n_l} = \mu^* + \Delta_{n_l} \tag{A3}$$

where Δ_{nl} is called the mean shift. Phoenix and Raj (1992) give a simple estimate for Δ_{n_l}

$$\Delta_{nl} = n_l^{-2/3} \left\{\frac{\rho}{3} s^{*\rho+2} + \frac{1-\rho}{3} s^{*2\rho+3}\right\}^{2/3} \{(\rho+1)^2 s^{*\rho}[1 - 2s^{*\rho+1}]\}^{-1/3} \tag{A4}$$

valid for $\rho \geqslant 4.5$. For smaller ρ's the mean shift is obtained from the more complex expression of Phoenix (1993), but with the new estimate for s^*. The latter takes into account the first order effects of the exclusion zone around fiber breaks; for $\rho = 2$, 3, and 4, it is given by $\Delta_{nl} = 0.9 n_l^{-2/3}$, $\Delta_{nl} = 0.582 n_l^{-2/3}$, and $\Delta_{nl} = 0.474 n_l^{-2/3}$, respectively.

We use the approximation to the standard deviation given by Phoenix and Raj (1992), but with the new estimate for s^*.

$$\gamma^*_{n_l} = \frac{s^*}{\sqrt{n_l}} \left[\frac{1}{12} + \frac{1}{6}\exp(-s^{*\rho+1}) - \frac{1}{4}\exp(-2s^{*\rho+1})\right]^{1/2}. \tag{A5}$$

Furthermore we include the correction to the standard deviation adapted to composites under GLS by Phoenix *et al.* (1995), from the results of classical bundles (McCartney and Smith, 1983),

$$\gamma^{**}_{n_l} = \gamma^*_{n_l} \left\{1 - 0.317 \left(\frac{\mu^*}{\gamma^*_{n_l}}\right)^2 \rho^{-2/3} e^{4/(3\rho)} n_l^{-4/3}\right\}^{1/2}. \tag{A6}$$

The correction term is important, since the number of fibers in a link $n_l \leqslant 100$ for most Weibull moduli of interest (e.g., for $\rho = 5$ and $n_l = 54$, the difference between $\gamma^*_{n_l}$ and $\gamma^{**}_{n_l}$ is 19%).